

# Model Predictive Control in Spacecraft Rendezvous and Soft Docking

Yaguang Yang\*

January 16, 2018

## Abstract

This paper discusses translation and attitude control in spacecraft rendezvous and soft docking. The target spacecraft orbit can be either circular or elliptic. The high fidelity model for this problem is intrinsically a nonlinear system but can be viewed as a linear time-varying system (LTV). Therefore, a model predictive control (MPC) based design is proposed to deal with the time-varying feature of the problem. A robust pole assignment method is used in the MPC-based design because of the following merits and/or considerations: (a) no overshoot of the relative position and attitude between the target and the chaser to achieve soft docking by placing all closed-loop poles in the negative real axis of the complex plan, which avoids oscillation of the relative position and attitude, in particular, in the final stage, (b) fast on-line computation, (c) modeling error tolerance, and (d) disturbance rejection. We will discuss these considerations and merits, and use a design simulation to demonstrate that the desired performance is indeed achieved.

**Keywords:** Attitude control, translation control, spacecraft rendezvous, reduced quaternion model, model predictive control.

---

\*Office of Research, NRC, 21 Church Street, Rockville, 20850. Email: yaguang.yang@verizon.net

# 1 Introduction

Spacecraft rendezvous is an important operation in many space missions. There are extensive research in this field and hundreds successful rendezvous missions, see, for example, the survey paper [1] and references therein. The entire rendezvous process can be divided into several phases, including phasing, close-range rendezvous, final approaching, and docking. In the early phase, the chaser fly to the target with the aid from the ground station and translation control is the main concern. For this purpose, the well-known Hill [2] or Clohessy and Wiltshire [3] equations are adequate for the control system design if the orbit is circular. But in the final approaching and docking phase, both translation and attitude control may be required. Moreover, we may need to consider the case that the orbit of the target spacecraft is not circular. To achieve this requirement, more complex models, for example, those discussed in [4, 5, 6], should be considered. Although these models are for more general purpose, they can be easily tailored for the use of spacecraft rendezvous and docking control.

The research of spacecraft rendezvous has attracted renewed interest in recent years as a result of new development in control theory and increased space missions involving rendezvous and soft docking. Various design methods have been considered for this control system design problem. For example, an adaptive output feedback control was proposed for this purpose in [7]; a multi-objective robust  $H_\infty$  control method was investigated in [8]; a Lyapunov differential equation approach was studied for elliptical orbital rendezvous with constrained controls [9]; a gain scheduled control of linear systems was applied to spacecraft rendezvous problem subject to actuator saturation [10]; and various control design methods were considered for 6 degree of freedom (DOF) spacecraft proximity operations [11, 12, 13, 14, 15]. All these methods have their merits in solving the challenging problem under various conditions, but none of them addressed a fundamental issue, i.e., to achieve the soft docking.

In this paper, we first carefully examine a newly proposed model derived in [6], then we determine the measurable variables and controllable inputs in the mission of the final approaching and docking phase, and make some reasonable assumptions that normally hold via engineering design. We also adopt a reduced quaternion concept proposed in [16] to slightly simplify the model (because of some merit discussed in [16, 17]). To make the general model useful for the control system design, thruster configuration is considered and modeled in a complete control system model. This complete model can be viewed either as a nonlinear model or a linear time-varying (LTV) model. We prefer to use the linear time-varying model because a linear system is easier to handle than a nonlinear system and the corresponding design methods are capable to consider the system performance which is very important as *soft docking may not allow overshoot in the relative position in the spacecraft rendezvous and docking phase*.

There are two popular methods that deal with linear time-varying control system design with the consideration of system performance. The first one is gain scheduling [18, 10] and the second one is model predictive control [19]. A simple analysis in [20] shows that the former is the most efficient when all time-varying parameters explicitly depends on time; and the later is more appropriate when many parameters depend implicitly on time. The rendezvous and docking model falls into the second category. Therefore, we propose a MPC-based method to design the rendezvous and docking control. Although several design methods, such as LQR,  $\mathbf{H}_\infty$ , and robust pole assignment, take the performance into the design consideration and can be the candidates for the MPC-based design, only robust pole assignment method can directly take overshoot into the design consideration because overshoot is directly related to the closed-loop pole positions [21]. In addition, robust pole assignment guarantees that the closed-loop poles are not sensitive to the parameter changes in the system [22] that is important given that the

system is time-varying. Moreover, robust pole assignment design minimizes an upper bound of  $\mathbf{H}_\infty$  norm which means that the design is robust to the modeling error and reduces the impact of disturbance torques on the system output [17]. Among many robust pole assignment algorithms, we suggest a globally convergent algorithm proposed in [23] because of its fast on-line computation and other merits [22]. We indicate that the closed-loop system is exponentially stable and use a design example to show the efficiency and effectiveness of the proposed method.

The remainder of the paper is organized as follows. Section 2 summarizes the complete rendezvous model of [6], simplifies the model for the use for rendezvous and soft docking control, and provides engineering design considerations for rendezvous and docking control. Section 3 discusses the MPC-based method for spacecraft control using robust pole assignment. Section 4 provides a design example and simulation result. Section 5 is the summary of conclusions of the paper.

## 2 Spacecraft model for rendezvous

In this section, we first introduce the model developed by Kristiansen et. al. in [6]. We also discuss the assumptions required from the application of final approaching and docking phase in the rendezvous process and derive a simplified model to be used in this paper. For the sake of simplicity, we denote a vector by bold symbol  $\mathbf{a}$  and its magnitude or 2-norm  $\|\mathbf{a}\|$  by normal font  $a$ . We make the following assumption throughout the paper.

**Assumption 1:** *Chaser and target can exchange information such as position, attitude and rotational rate in real time.*

This assumption can be achieved by engineering design.

### 2.1 The model for translation dynamics

As shown in Figure 1, the inertial frame is defined by standard earth-centered inertial (ECI) frame  $\mathcal{F}_i$  [24]. Let  $\mathbf{r}_t$  be the vector from the Earth center to the center of the mass of the target and  $\mathbf{r}_c$  be the vector from the Earth center to the center of the mass of the chaser. Let the angular momentum vector of the target orbit be denoted by  $\mathbf{h} = \mathbf{r}_t \times \dot{\mathbf{r}}_t$ . The orbital frame is the standard local vertical local horizontal (LVLH) frame  $\mathcal{F}_t$  centered on the target with the basis vectors of the frame  $\mathbf{e}_r = \mathbf{r}_t/r_t$ ,  $\mathbf{e}_h = \mathbf{h}/h$ , and  $\mathbf{e}_\theta = \mathbf{e}_h \times \mathbf{e}_r$ . The relative position vector between a target and a chaser is defined by

$$\mathbf{p} = \mathbf{r}_c - \mathbf{r}_t = x\mathbf{e}_r + y\mathbf{e}_\theta + z\mathbf{e}_h. \quad (1)$$

$\mathbf{p}$  is available in real time if GPS is installed in both spacecraft and Assumption 1 holds. The body frames of the target and the chaser,  $\mathcal{F}_{tb}$  and  $\mathcal{F}_{cb}$ , have their origins at their centers of mass and their coordinate vectors are their principal axes of the inertia. Let  $\gamma$  be the true anomaly of the target,  $m_t$  be the mass of the target and  $m_c$  be the mass of the chaser,  $\mu$  be the geocentric gravitational constant. Then, the nonlinear *relative position dynamics* can be expressed in the target frame as [6]:

$$m_c \ddot{\mathbf{p}} + \mathbf{C}_t(\dot{\gamma}) \dot{\mathbf{p}} + \mathbf{D}_t(\dot{\gamma}, \ddot{\gamma}, r_c) \mathbf{p} + \mathbf{n}_t(r_c, r_t) = \mathbf{f}_c + \mathbf{f}_d, \quad (2)$$

where

$$\mathbf{C}_t(\dot{\gamma}) = 2m_c \dot{\gamma} \begin{bmatrix} 0 & -1 & 0 \\ 1 & 0 & 0 \\ 0 & 0 & 0 \end{bmatrix} \quad (3)$$

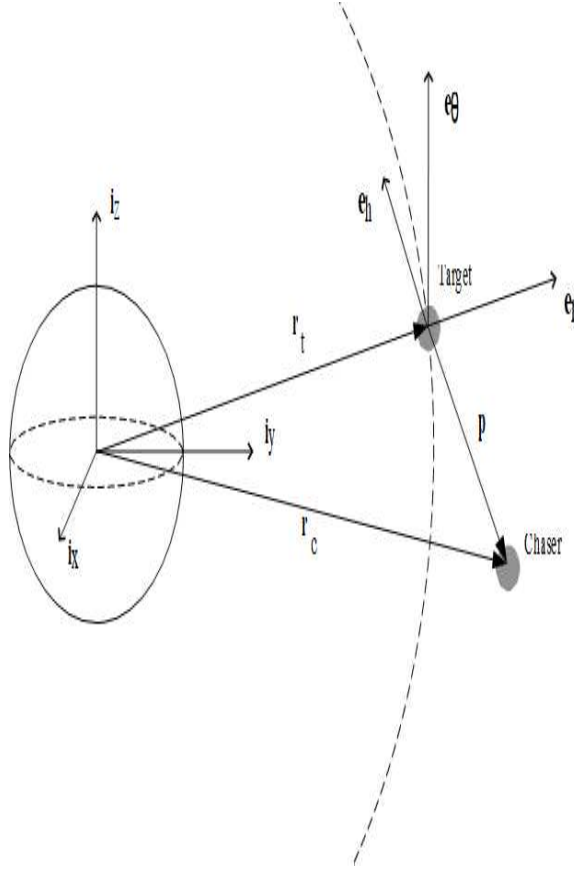


Figure 1: Coordinate Frame.

$$\mathbf{D}_t(\dot{\gamma}, \ddot{\gamma}, r_c) = m_c \begin{bmatrix} \frac{\mu}{r_c^3} - \dot{\gamma} & -\ddot{\gamma} & 0 \\ \ddot{\gamma} & \frac{\mu}{r_c^3} - \dot{\gamma} & 0 \\ 0 & 0 & \frac{\mu}{r_c^3} \end{bmatrix} \quad (4)$$

$$\mathbf{n}_t(r_c, r_t) = m_c \mu [r_t/r_c^3 - 1/r_t^2, 0, 0]^T, \quad (5)$$

$\mathbf{f}_c$  is the control force vector, and  $\mathbf{f}_d$  is the disturbance force vector, both are applied in chaser's body frame. It is worthwhile to note that

$$\mathbf{n}_t(r_c, r_t)|_{r_c=r_t} = \mathbf{0}. \quad (6)$$

Also, according to Assumption 1,  $\mathbf{C}_t(\dot{\gamma})$ ,  $\mathbf{D}_t(\dot{\gamma}, \ddot{\gamma}, r_c)$  and  $\mathbf{n}_t(r_c, r_t)$  are known but are time-varying.

## 2.2 The model for attitude dynamics

Let the unit quaternion  $\bar{\mathbf{q}} = [q_0, \mathbf{q}^T]^T$  be the relative attitude of the target and chaser, where

$$\mathbf{q}^T = [q_1, q_2, q_3]. \quad (7)$$

The inverse of the quaternion is defined in [24] as  $\bar{\mathbf{q}}^{-1} = [q_0, -\mathbf{q}^T]^T$ . Let  $\bar{\mathbf{q}}_{i,cb} = [q_{c0}, q_{c1}, q_{c2}, q_{c3}]$  be the relative quaternion of from chaser's body frame to the inertial frame, and  $\bar{\mathbf{q}}_{i,tb} = [q_{t0}, q_{t1}, q_{t2}, q_{t3}]$  be the the relative quaternion of from target's body frame to the inertial frame. Notice that  $\bar{\mathbf{q}}_{i,cb}$  is measurable from the chaser and  $\bar{\mathbf{q}}_{i,tb}$  is measurable from the target. Using the Assumption 1, equation (7.2.14) of [25], and equation (45b) of [24], we have

$$\bar{\mathbf{q}} = \bar{\mathbf{q}}_{i,cb}^{-1} \bar{\mathbf{q}}_{i,tb} = \begin{bmatrix} q_{t0} & -q_{t1} & -q_{t2} & -q_{t3} \\ q_{t1} & q_{t0} & q_{t3} & -q_{t2} \\ q_{t2} & -q_{t3} & q_{t0} & q_{t1} \\ q_{t3} & q_{t2} & -q_{t1} & q_{t0} \end{bmatrix} \begin{bmatrix} q_{c0} \\ -q_{c1} \\ -q_{c2} \\ -q_{c3} \end{bmatrix}, \quad (8)$$

which, according to Assumption 1, is measurable. The relative angular velocity between frames  $\mathcal{F}_{cb}$  and  $\mathcal{F}_{tb}$  expressed in frame  $\mathcal{F}_{cb}$  is given by

$$\boldsymbol{\omega} = \boldsymbol{\omega}_{i,cb}^{cb} - \mathbf{R}_{tb}^{cb} \boldsymbol{\omega}_{i,tb}^{tb} = [\omega_1, \omega_2, \omega_3]^T, \quad (9)$$

where  $\boldsymbol{\omega}_{i,cb}^{cb}$  is the angular velocity of the chaser body frame relative to the inertial frame expressed in the chaser body frame, which is measurable from the chaser;  $\boldsymbol{\omega}_{i,tb}^{tb}$  is the angular velocity of the target body frame relative to the inertial frame expressed in the target body frame, which is measurable from the target;  $\mathbf{R}_{tb}^{cb}$  is the rotational matrix from  $\mathcal{F}_{tb}$  to  $\mathcal{F}_{cb}$  which is an equivalent rotation of  $\bar{\mathbf{q}}$  and can be expressed as [24, eq. (43)]

$$\mathbf{R}_{tb}^{cb} = (q_0^2 - \mathbf{q}^T \mathbf{q}) \mathbf{I} + 2\mathbf{q}\mathbf{q}^T - 2q_0 \mathbf{S}(\mathbf{q}), \quad (10)$$

where  $\mathbf{S}(\mathbf{q}) = \mathbf{q} \times$  is a cross product operator. Using Assumption 1 again, we conclude that  $\boldsymbol{\omega}$  is available from measurements. Let  $\mathbf{J}_c$  and  $\mathbf{J}_t$  be the inertia matrices of the chaser and the target, respectively. The relative attitude dynamics is given in chaser's frame as [6, 12]:

$$\mathbf{J}_c \dot{\boldsymbol{\omega}} + \mathbf{C}_r(\boldsymbol{\omega}, \mathbf{q}) \boldsymbol{\omega} + \mathbf{n}_r(\boldsymbol{\omega}, \mathbf{q}) = \mathbf{t}_c + \mathbf{t}_d, \quad (11)$$

where  $\mathbf{t}_c$  and  $\mathbf{t}_d$  are control torque and disturbance torque respectively, both are applied to the chaser's body frame,  $\mathbf{C}_r(\boldsymbol{\omega})$  and  $\mathbf{n}_r(\boldsymbol{\omega})$  are given as follows:

$$\mathbf{C}_r(\boldsymbol{\omega}, \mathbf{q}) = \mathbf{J}_c \mathbf{S}(\mathbf{R}_{tb}^{cb} \boldsymbol{\omega}_{i,tb}^{tb}) + \mathbf{S}(\mathbf{R}_{tb}^{cb} \boldsymbol{\omega}_{i,tb}^{tb}) \mathbf{J}_c - \mathbf{S}(\mathbf{J}_c(\boldsymbol{\omega} + \mathbf{R}_{tb}^{cb} \boldsymbol{\omega}_{i,tb}^{tb})), \quad (12)$$

$$\mathbf{n}_r(\boldsymbol{\omega}, \mathbf{q}) = \mathbf{S}(\mathbf{R}_{tb}^{cb} \boldsymbol{\omega}_{i,tb}^{tb}) \mathbf{J}_c \mathbf{R}_{tb}^{cb} \boldsymbol{\omega}_{i,tb}^{tb} - \mathbf{J}_c \mathbf{R}_{tb}^{cb} \mathbf{J}_t^{-1} \mathbf{S}(\boldsymbol{\omega}_{i,tb}^{tb}) \mathbf{J}_t \boldsymbol{\omega}_{i,tb}^{tb}. \quad (13)$$

At the end of the docking phase, the rotation matrix satisfies  $\mathbf{R}_{tb}^{cb} = \mathbf{I}$ .

For attitude dynamics, we use the reduced quaternion as proposed in [16] which is given as follows<sup>1</sup>:

$$\begin{aligned} \dot{\bar{\mathbf{q}}} &= \begin{bmatrix} \dot{q}_1 \\ \dot{q}_2 \\ \dot{q}_3 \end{bmatrix} = \frac{1}{2} \begin{bmatrix} \sqrt{1 - q_1^2 - q_2^2 - q_3^2} & -q_3 & q_2 \\ q_3 & \sqrt{1 - q_1^2 - q_2^2 - q_3^2} & -q_1 \\ -q_2 & q_1 & \sqrt{1 - q_1^2 - q_2^2 - q_3^2} \end{bmatrix} \begin{bmatrix} \omega_1 \\ \omega_2 \\ \omega_3 \end{bmatrix} \\ &= \frac{1}{2} \mathbf{T} \boldsymbol{\omega}. \end{aligned} \quad (14)$$

<sup>1</sup> In the final approaching and docking phase, the attitude error between chaser and target is very small, the quaternion is far away from the only singular point of the reduced quaternion.

### 2.3 A complete model for rendezvous and docking

Let

$$\mathbf{r} = \dot{\mathbf{p}}, \quad (15)$$

which can be approximated by  $\dot{\mathbf{p}} \approx \Delta \mathbf{p} / \Delta t$ . Now, we can summarize the result by combining equations (15), (2), (11), and (14), which yields

$$\dot{\mathbf{x}} = \begin{bmatrix} \dot{\mathbf{p}} \\ \dot{\mathbf{r}} \\ \dot{\mathbf{q}} \\ \dot{\boldsymbol{\omega}} \end{bmatrix} = \begin{bmatrix} \mathbf{0} & \mathbf{I} & \mathbf{0} & \mathbf{0} \\ -\frac{1}{m_c} \mathbf{D}_t & -\frac{1}{m_c} \mathbf{C}_t & \mathbf{0} & \mathbf{0} \\ \mathbf{0} & \mathbf{0} & \mathbf{0} & \frac{1}{2} \mathbf{T} \\ \mathbf{0} & \mathbf{0} & \mathbf{0} & -\mathbf{J}_c^{-1} \mathbf{C}_r \end{bmatrix} \begin{bmatrix} \mathbf{p} \\ \mathbf{r} \\ \mathbf{q} \\ \boldsymbol{\omega} \end{bmatrix} - \begin{bmatrix} \mathbf{0} \\ \frac{1}{m_c} \mathbf{n}_t \\ \mathbf{0} \\ \mathbf{J}_c^{-1} \mathbf{n}_r \end{bmatrix} + \begin{bmatrix} \mathbf{0} \\ \frac{1}{m_c} \mathbf{f}_c \\ \mathbf{0} \\ \mathbf{J}_c^{-1} \mathbf{t}_c \end{bmatrix}. \quad (16)$$

Since  $\mathbf{D}_t$ ,  $\mathbf{C}_t$ ,  $\mathbf{T}$ ,  $\mathbf{C}_r$ ,  $\mathbf{n}_t$ , and  $\mathbf{n}_r$  depend on  $\mathbf{q}$ ,  $\boldsymbol{\omega}$ ,  $r_c$ ,  $r_t$ ,  $\gamma$  which are all time-varying, equation (16) can be treated as a linear time-varying system.

For spacecraft rendezvous and docking, the control forces and torques are provided by thruster systems. It is well-known that the control force vector and control torque vector depend on the thruster configurations and many configurations are reported in different systems, for example, [26, 27, 28]. Let  $\mathbf{F}_a$  and  $\mathbf{T}_a$  be the thruster configuration related matrices that define the control force vector and control torque vector, i.e.,

$$\mathbf{f}_c = \mathbf{F}_a \mathbf{f}_a, \quad \mathbf{t}_c = \mathbf{T}_a \mathbf{f}_a, \quad (17)$$

where  $\mathbf{f}_a$  is the vector of forces generated by thrusters. Substituting (17) into (16), we have

$$\begin{aligned} \dot{\mathbf{x}} &= \begin{bmatrix} \dot{\mathbf{p}} \\ \dot{\mathbf{r}} \\ \dot{\mathbf{q}} \\ \dot{\boldsymbol{\omega}} \end{bmatrix} = \begin{bmatrix} \mathbf{0} & \mathbf{I} & \mathbf{0} & \mathbf{0} \\ -\frac{1}{m_c} \mathbf{D}_t & -\frac{1}{m_c} \mathbf{C}_t & \mathbf{0} & \mathbf{0} \\ \mathbf{0} & \mathbf{0} & \mathbf{0} & \frac{1}{2} \mathbf{T} \\ \mathbf{0} & \mathbf{0} & \mathbf{0} & -\mathbf{J}_c^{-1} \mathbf{C}_r \end{bmatrix} \begin{bmatrix} \mathbf{p} \\ \mathbf{r} \\ \mathbf{q} \\ \boldsymbol{\omega} \end{bmatrix} - \begin{bmatrix} \mathbf{0} \\ \frac{1}{m_c} \mathbf{n}_t \\ \mathbf{0} \\ \mathbf{J}_c^{-1} \mathbf{n}_r \end{bmatrix} + \begin{bmatrix} \mathbf{0} \\ \frac{1}{m_c} \mathbf{F}_a \\ \mathbf{0} \\ \mathbf{J}_c^{-1} \mathbf{T}_a \end{bmatrix} \mathbf{f}_a \\ &= \mathbf{A}(t) \mathbf{x} - \mathbf{n}_d(t) + \mathbf{B} \mathbf{f}_a. \end{aligned} \quad (18)$$

Assuming that the chaser's mass change due to fuel consumption is negligible, the matrix  $\mathbf{B}$  is then a constant. For illustrative purpose, in the rest of the discussion, we assume that the thrusters have the configuration considered in [12] which is described in Figure 2. But the same idea can be used in other thruster configurations. Therefore, we have

$$\mathbf{F}_a = \begin{bmatrix} 0 & 0 & 1 & -1 & 0 & 0 \\ 0 & 0 & 0 & 0 & 1 & -1 \\ 1 & -1 & 0 & 0 & 0 & 0 \end{bmatrix}, \quad (19)$$

and

$$\mathbf{T}_a = \begin{bmatrix} \frac{L_2}{2} & \frac{L_2}{2} & 0 & 0 & \frac{L_3}{2} & \frac{L_3}{2} \\ -\frac{L_1}{2} & -\frac{L_1}{2} & \frac{L_3}{2} & \frac{L_3}{2} & 0 & 0 \\ 0 & 0 & -\frac{L_2}{2} & -\frac{L_2}{2} & \frac{L_1}{2} & \frac{L_1}{2} \end{bmatrix}. \quad (20)$$

It is easy to check that the following matrix

$$\mathbf{G} := \begin{bmatrix} \mathbf{F}_a \\ \mathbf{T}_a \end{bmatrix} \quad (21)$$

is full row rank matrix. As a matter of fact, in engineer practice, thruster configuration should always be designed to be able to fully control the translation and attitude operations. Therefore, we may make the following assumption in the rest of the paper:

**Assumption 2:** The configuration matrix  $\mathbf{G}$  is always a full row rank matrix.

### 3 Control system design using model predictive control

Although it is not always straightforward to analyze the close-loop stability for MPC control system designs, the following theorem (cf. [29, pages 117-119]) provides a nice sufficient stability criterion for the linear time-varying system.

**Theorem 3.1** *Suppose for a closed-loop linear time-varying system  $\dot{\mathbf{x}} = \mathbf{A}(t)\mathbf{x}$  with  $\mathbf{A}(t)$  continuously differentiable there exist finite positive constants  $\alpha, \mu$  such that, for all  $t$ ,  $\|\mathbf{A}(t)\| \leq \alpha$  and every pointwise eigenvalue of  $\mathbf{A}(t)$  satisfies  $\mathcal{R}_e[\lambda(t)] \leq -\mu$ . Then there exists a positive constant  $\beta$  such that if the time derivative of  $\mathbf{A}(t)$  satisfies  $\|\dot{\mathbf{A}}(t)\| \leq \beta$  for all  $t$ , the state equation is uniformly exponentially stable.*

This theorem is the theoretical base for us to use the MPC design for the linear time-varying system. It is also worthwhile to indicate the following facts: the robust pole assignment design can easily achieve the condition that the closed-loop system at every fixed time satisfies  $\mathcal{R}_e[\lambda(t)] \leq -\mu$ , which is required in Theorem 3.1; for any time between the fixed sampling time, robust pole assignment design minimizes the sensitivity of the closed-loop poles to the parameter changes [22]; moreover, it reduces the impact of disturbance torques [17]. Among various pole assignment algorithms, we choose the one proposed in [30, 23] because it needs the shortest computation time among several other popular algorithms [22], a critical requirement for MPC design.

We will divide the control force into two parts. The first part is used to cancel  $\mathbf{n}_d(t)$  in (18). This can be achieved simply by solving the following linear system of equations.

$$\begin{bmatrix} \mathbf{F}_a \\ \mathbf{T}_a \end{bmatrix} \mathbf{u}_1 = \mathbf{G} \mathbf{u}_1 = \begin{bmatrix} \mathbf{n}_t(t) \\ \mathbf{n}_r(t) \end{bmatrix}, \quad (22)$$

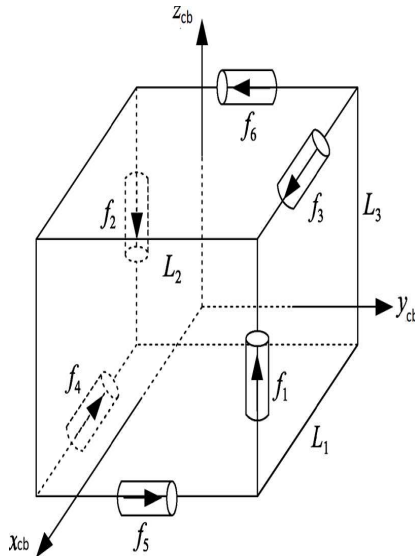


Figure 2: Thruster configuration.

which gives

$$\mathbf{u}_1 = \mathbf{G}^\dagger \begin{bmatrix} \mathbf{n}_t(t) \\ \mathbf{n}_r(t) \end{bmatrix} := \mathbf{G}^\dagger \mathbf{n}, \quad (23)$$

where  $\mathbf{G}^\dagger$  is pseud-inverse of  $\mathbf{G}$ . In our example, equations (19) and (20) implies  $\mathbf{G}^\dagger = \mathbf{G}^{-1}$ .

The design of second part of the thruster force  $\mathbf{u}_2$  is based on the following linear time-varying system:

$$\dot{\mathbf{x}} = \mathbf{A}(t)\mathbf{x} + \mathbf{B}\mathbf{u}_2, \quad (24)$$

where  $\mathbf{x}$ ,  $\mathbf{A}(t)$ , and  $\mathbf{B}$  are defined as in (18). At every sampling time  $t$ ,  $\mathbf{A}(t)$  is evaluated based on the measurable variables. The robust pole assignment algorithm of [23] is called to get the feedback matrix

$$\mathbf{u}_2 = \mathbf{K}(t)\mathbf{x}.$$

The feedback force  $\mathbf{f}_a = \mathbf{u}_1 + \mathbf{u}_2$  is applied to the linear time-varying system (18). The new variables are measured and the next  $\mathbf{A}(t)$  is evaluated in the next sampling time, and the process is repeated. To avoid the overshoot of relative position and relative attitude in the rendezvous and docking process, the closed-loop poles should be assigned on the negative real axis, i.e., all the poles should be negative and real.

The MPC algorithm using robust pole assignment is summarized as follows:

### Algorithm 3.1

*Data:*  $\mu, m_c, L_1, L_2, L_3, \mathbf{J}_c, \mathbf{J}_t, \mathbf{F}_a, \mathbf{T}_a$ , and  $\mathbf{B}$ .

*Initial condition:* At time  $t_0$ , take the measurements  $\gamma = \gamma_0, \mathbf{r}_c, \mathbf{r}_t, \bar{\mathbf{q}}_{i,tb}, \bar{\mathbf{q}}_{i,cb}, \boldsymbol{\omega}_{i,cb}^{cb}, \boldsymbol{\omega}_{i,tb}^{tb}$ , calculate  $\mathbf{p}, \mathbf{r}, \mathbf{q}, \mathbf{R}_{tb}^{cb}, \boldsymbol{\omega}$ , which gives  $\mathbf{x} = \mathbf{x}_0$ .

*Step 1:* Update  $\mathbf{n}_t(r_c, r_t), \mathbf{n}_r(\boldsymbol{\omega}, \mathbf{q})$  which gives  $\mathbf{n}_d(t)$ ; update  $\mathbf{A}(t)$  using  $\mathbf{D}_t(\dot{\gamma}, \ddot{\gamma}, \mathbf{r}_c), \mathbf{C}_t(\dot{\gamma}), \mathbf{C}_r(\boldsymbol{\omega}, \mathbf{q})$ , and  $\mathbf{T}(\mathbf{q})$ .

*Step 2:* Calculate the gain  $\mathbf{K}$  for the linear time-varying system (24) using robust pole assignment algorithm implemented as `robpole` (cf. [23]).

*Step 3:* Apply the controlled thruster force  $\mathbf{f}_a = \mathbf{u}_1 + \mathbf{u}_2 = \mathbf{G}^\dagger \mathbf{n} + \mathbf{K}\mathbf{x}$  to (18).

*Step 4:* Take the measurements  $\gamma, \mathbf{r}_c, \mathbf{r}_t, \bar{\mathbf{q}}_{i,tb}, \bar{\mathbf{q}}_{i,cb}, \boldsymbol{\omega}_{i,cb}^{cb}, \boldsymbol{\omega}_{i,tb}^{tb}$ , calculate  $\mathbf{p}, \mathbf{r}, \mathbf{q}, \mathbf{R}_{tb}^{cb}, \boldsymbol{\omega}$ , which gives  $\mathbf{x}$ . Go back to Step 1.

The most important step of the algorithm is to call a robust pole assignment algorithm `robpole` (cf. [23, 30]). Let the desired closed-loop eigenvalue set be  $\boldsymbol{\Lambda} = \text{diag}(\lambda_i)$  and its corresponding eigenvector matrix be  $\mathbf{X} = [\mathbf{x}_1, \dots, \mathbf{x}_n]$  with  $\|\mathbf{x}_i\| = 1$  such that

$$(\mathbf{A} + \mathbf{BK})\mathbf{X} = \det(\mathbf{X})\boldsymbol{\Lambda}. \quad (25)$$

The algorithm of `robpole` is to maximize robustness measurement of  $\det(\mathbf{X})$  which measures the size of box spanned by the eigenvector matrix  $\mathbf{X}$  [22]. That is

$$\max_{\|\mathbf{x}_i\|=1, i=1, \dots, n} \det(\mathbf{X}) \quad \text{s.t.} \quad (\mathbf{A} + \mathbf{BK})\mathbf{X} = \mathbf{X}\boldsymbol{\Lambda}. \quad (26)$$

The algorithm can be summarized as follows:



**Algorithm 3.2** robpole

Data:  $\mathbf{A}$ ,  $\mathbf{B}$ , and diagonal matrix  $\mathbf{\Lambda} = \text{diag}(\lambda_i)$  with  $\lambda_i$  being the desired closed-loop poles.

Step 1: QR decomposition for  $\mathbf{B}$  yields orthogonal  $\mathbf{Q} = [\mathbf{Q}_0 \ \mathbf{Q}_1]$  and triangular  $\mathbf{R}$  such that

$$\mathbf{B} = [\mathbf{Q}_0 \ \mathbf{Q}_1] \begin{bmatrix} \mathbf{R} \\ \mathbf{0} \end{bmatrix}. \quad (27)$$

Step 2: QR decomposition for  $(\mathbf{A}^T(t) - \lambda_i \mathbf{I})\mathbf{Q}_1$  yields orthogonal  $\mathbf{V} = [\mathbf{V}_{0i} \ \mathbf{V}_{1i}]$  and triangular  $\mathbf{Y}$  such that

$$(\mathbf{A}^T(t) - \lambda_i \mathbf{I})\mathbf{Q}_1 = [\mathbf{V}_{0i} \ \mathbf{V}_{1i}] \begin{bmatrix} \mathbf{Y} \\ \mathbf{0} \end{bmatrix}, \quad i = 1, \dots, n. \quad (28)$$

Step 3: Cyclically select one real or a pair of (real or complex conjugate) unit length eigenvectors such that  $\mathbf{x}_i \in \mathcal{S}_i = \text{span}(\mathbf{V}_{1i})$  and the robustness measure  $\det(\mathbf{X})$  is maximized.

Step 4: The feedback matrix is given by

$$\mathbf{K} = \mathbf{R}^{-1} \mathbf{Q}_0^T (\mathbf{X} \mathbf{\Lambda} \mathbf{X}^{-1} - \mathbf{A}(t)). \quad (29)$$

**Remark 3.1** It is worthwhile to emphasize that  $\mathbf{B}$  in (24) is a constant matrix. Therefore, Step 1 can be calculated off-line, which saves a lot of computational burden for the MPC control scheme.

In [17], it is shown that maximizing  $\det(\mathbf{X})$  is equivalent to minimizing an upper-bound of  $\mathbf{H}_\infty$  norm of the closed-loop system. Therefore, the design is insensitive to modeling error. Moreover, maximizing  $\det(\mathbf{X})$  amounts to minimizing the an upper-bound of the gain of the channel from disturbance input to the output. This can be seen as follows: Assume that system (24) with disturbance  $\mathbf{f}_d$  is

$$\dot{\mathbf{x}} = \mathbf{A}(t)\mathbf{x} + \mathbf{B}\mathbf{u} + \mathbf{f}_d,$$

and its output vector is defined by

$$\mathbf{y} = \mathbf{x}..$$

Since  $\mathbf{u} = \mathbf{K}\mathbf{x}$ , taking the Laplace transformation gives

$$\mathbf{Y}(s) = (s\mathbf{I} - (\mathbf{A} + \mathbf{BK}))^{-1} \mathbf{f}_d(s) = \mathbf{X}(s\mathbf{I} - \mathbf{\Lambda})^{-1} \mathbf{X}^{-1} \mathbf{f}_d(s).$$

This gives

$$\|\mathbf{Y}(s)\| \leq \|(s\mathbf{I} - \mathbf{\Lambda})^{-1}\| \cdot \|\mathbf{X}\| \cdot \|\mathbf{X}^{-1}\| \cdot \|\mathbf{f}_d(s)\| \quad (30)$$

where  $\|(s\mathbf{I} - \mathbf{\Lambda})^{-1}\|$  is a constant,  $\|\mathbf{f}_d(s)\|$  is the unknown disturbance, and  $\kappa := \|\mathbf{X}\| \cdot \|\mathbf{X}^{-1}\| = \sigma_1/\sigma_n$  ( $\sigma_1$  and  $\sigma_n$  are the maximum and minimum singular values of  $\mathbf{X}$ ). According to [17], maximizing  $\det(\mathbf{X})$  implies minimizing the upper bound of  $\kappa = \|\mathbf{X}\| \cdot \|\mathbf{X}^{-1}\|$ . Therefore, from (30), we conclude that the robust pole assignment design reduces the impact of  $\mathbf{f}_d$  on the output of  $\mathbf{Y}$ , which means that the design has good disturbance rejection property.

Applying Theorem 3.1, Yang [20] provides some moderate conditions for uniformly exponential stability for a class of the MPC designs, which can easily be extended to Algorithm 3.1.

**Theorem 3.2 ([20])** *Let the prescribed closed-loop eigenvalues be distinct and  $\mathcal{R}_e[\lambda_i(t)] \leq -\mu$  for some  $\mu > 0$ , and the time dependent variables in LTV system  $(\mathbf{A}(t), \mathbf{B}(t))$  and their derivatives be bounded. Then, the closed-loop time-varying system (16) with the robust pole assignment control obtained by Algorithm 3.1 is uniformly exponentially stable.*

## 4 Simulation test

In this section, we present an simulation test example to support the design idea. We use the simulation example of [12] and all the parameters used in that paper. We compare the simulation results of the two designs to demonstrate the superiority of the proposed design.

First, the physics constants, such as, gravitational constant  $\mu = 3.986004418 * 10^{14} m^3 / (kg \cdot s^2)$ , Earth radius 6371000 m, are from [31]. The rest parameters are from [12]: the target spacecraft orbit is circular and the altitude is 250 km,  $L_1 = L_2 = L_3 = 2$  m, the mass of the chaser is 10 kg and its inertia matrix is  $\mathbf{J}_c = \text{diag}[10, 10, 10] kg \cdot m^2$ , the mass of the target 10 kg and its inertia matrix is given as

$$\mathbf{J}_t = \begin{bmatrix} 10 & 2.5 & 3.5 \\ 2.5 & 10 & 4.5 \\ 3.5 & 4.5 & 10 \end{bmatrix} kg \cdot m^2,$$

$\mathbf{F}_a$  is given in (19),  $\mathbf{T}_a$  is given in (20). The initial condition is set as  $\mathbf{p}(0) = [10, -10, 10]^T m$ ,  $\mathbf{d}(0) = [5, -4, 4]^T m/s$ ,  $\bar{\mathbf{q}}(0) = [0.3772, -0.4329, 0.6645, 0.4783]^T$ ,  $\boldsymbol{\omega}(0) = [0, 0, 0]^T rad/s$ .

To avoid the overshoot in relative distance and relative attitude to guarantee the soft docking, we should avoid the oscillation. Therefore, the proposed closed loop poles are set to

$$-0.1 - 0.2 - 0.15 - 0.25 - 0.3 - 0.35 - 0.4 - 0.45 - 0.5 - 0.55 - 0.6 - 0.65$$

Applying the on-line algorithm 3.1 to this problem again, we performed the simulation of the closed-loop response. The results are shown in Figures 3 - 5. Fig. 3 is the response of relative position between the chaser and the target and Fig. 4 is the response of relative attitude between the chaser and the target. These figures show that the design successfully avoid the oscillation in the docking process and achieved the soft docking. Fig. 5 is the forces in 6 thrusters used in this docking process, the maximum forces is about 31 Newton, which is smaller than the maximum forces used in the design of [12], which is in the range of 360 Newton.

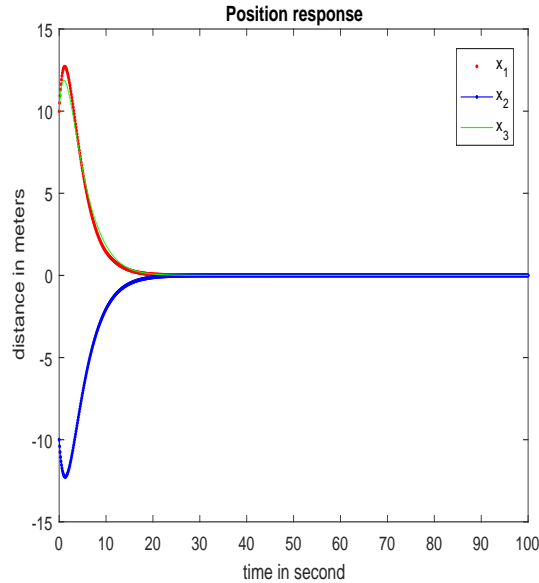


Figure 3: Position response.

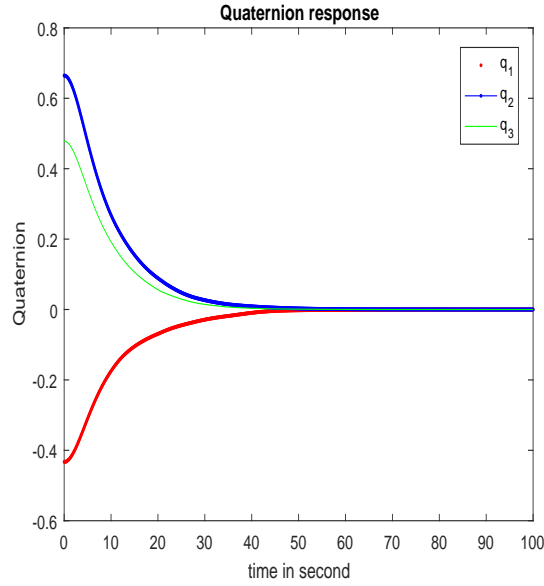


Figure 4: Attitude response.

Comparing to the simulation tests in [7, 8, 9, 10, 11, 12, 13, 14, 15], the simulation using the proposed method is the only one that does not have oscillation in all these responses, which is a clear indication that the design achieves soft docking.

To verify that the design is insensitive to the modeling error on the performance and the design reduces the impact of disturbance torques, we consider the first set of prescribed closed-loop eigenvalues with (a) randomly generated modeling errors in all entries of  $\mathbf{J}_t$  and  $\mathbf{J}_c$  for up to  $1kg \cdot m^2$ , (b) randomly generated installation errors in thruster location  $L_1$ ,  $L_2$ , and

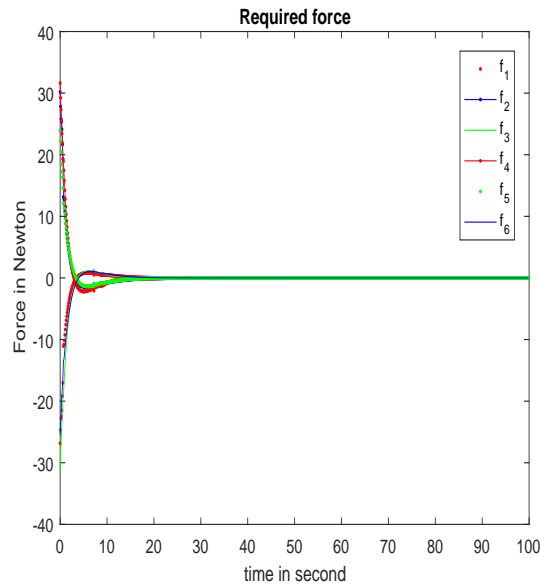


Figure 5: Required forces.

$L_3$  for up to  $0.01m$ , and (c) randomly generated disturbance with magnitude for up to  $10\% \mathbf{B} * \mathbf{F} * \|\mathbf{x}(t)\|$  for all  $t > 0$ . The system is controlled by using the controller designed in this section without the information on the randomly generated modeling and installation error and randomly generated disturbances. The performance of the position responses and attitude responses for 100 randomly generated problems described above is provided in Figures 6 and 7. Clearly, the performance of position and attitude responses is insensitive to the modeling error and disturbance torques.

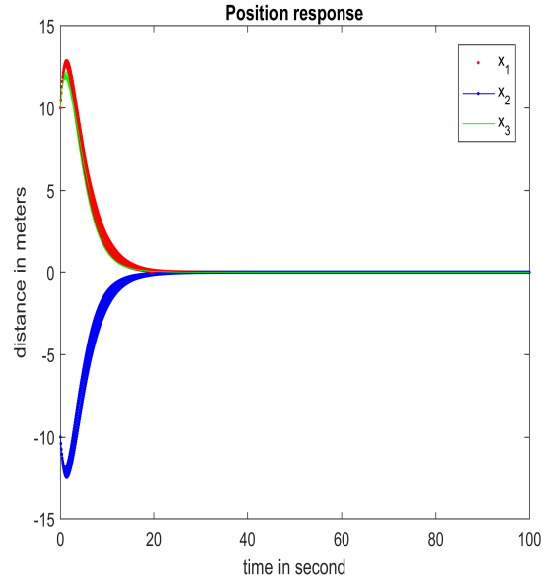


Figure 6: Position response for randomly generated 100 problems.

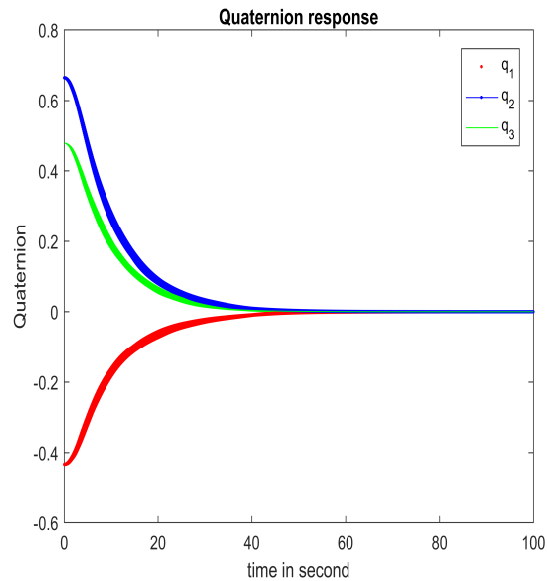


Figure 7: Attitude response for randomly generated 100 problems.

## 5 Conclusions

In this paper, we proposed an MPS-based design method for translation and attitude combined control in spacecraft rendezvous and soft docking. A robust pole assignment design is used in the MPS-based method, which enjoys several nice features: (a) all closed-loop poles are negative real which guarantees the strict requirement of soft docking, (b) on-line computation is moderate and all intermediate solutions are feasible, (c) the design is insensitive to the effects of the modeling error on the performance, and (d) the design reduces the impact of disturbance torques. A simulation example is included to demonstrate the effectiveness and the efficiency of the proposed design.

## References

- [1] Y. Luo, J. Zhang, and G. Tang, Survey of orbital dynamics and control of space rendezvous, Chinese Journal of Aeronautics, Vol. 27, No. 1, 2014, pp. 1-11.
- [2] G. W. Hill, Researches in lunar theory, American Journal of Mathematics, Vol. 1, No. 1, 1878, pp. 5-26.
- [3] Clohessy, W. H. and Wiltshire, R. S., Terminal guidance system for satellite rendezvous, Journal of Aerospace Sciences, Vol. 27, No. 9, 1960, pp. 653-658.
- [4] P. K. C. Wang, and F. Y. Hadaegh, Coordination and control of multiple microspacecraft moving in formation, Journal of Astronautical Sciences, Vol. 44, No. 3, 1996, pp. 315-355.
- [5] Pan, H. and Kapila, V., Adaptive Nonlinear Control for Spacecraft Formation Flying with Coupled Translational and Attitude Dynamics, Proceedings of the Conference on Decision and Control, Orlando, FL, 2001.
- [6] R. Kristiansen, E. I. Grotli, P. J. Nicklasso, and J. T. Gravdahl, A model of relative translation and rotation in leader-follower spacecraft formations, Modeling, Identification and Control, 28(1) 2007, pp. 3-13.
- [7] P. Singla, K. Subbarao, J. L. Junkins, Adaptive output feedback control for spacecraft rendezvous and docking under measurement uncertainty, Journal of Guidance Control and Dynamics, 29(4), 2006, 892-902.
- [8] H. Gao, X. Yang, and P. Shi, Multi-Objective Robust  $H_\infty$  Control of Spacecraft Rendezvous, IEEE Transactions on Control Systems Technology, Vol. 17, No. 4, 2009, pp. 794-802.
- [9] B. Zhou, Z. Lin, G. Duan, Lyapunov differential equation approach to elliptical orbital rendezvous with constrained controls, Journal of Guidance Control and Dynamics, 34(2), 2011, 892-902.
- [10] B. Zhou, Q. Wang, Z. Lin, G. Duan, Gain scheduled control of linear systems subject to actuator saturation with application to spacecraft rendezvous, IEEE Transactions on Control Systems Technology, 22(5), 2014, pp. 2031-2038.
- [11] L. Sun; W. Huo, 6-DOF integrated adaptive backstepping control for spacecraft proximity operations, IEEE Transactions on Aerospace and Electronic Systems, 51(3), 2015, pp. 2433-2443.

- [12] F. Zhang and G. Duan, Integrated relative position and attitude control of spacecraft in proximity operation missions, *International Journal of Automation and Computing*, 9(4), 2012, pp. 342-351.
- [13] R. Kristiansena, P. J. Nicklassona, J. T. Gravdahlb, Spacecraft coordination control in 6DOF: Integrator backstepping vs passivity-based control, *Automatica*, Vol. 44, No. 11, 2008, pp. 2896-2901.
- [14] H. Sun, S. Lia, S. Fei, A composite control scheme for 6DOF spacecraft formation control, *Acta Astronautica*, Vol. 69, No. 7-8, 2011, pp. 595-611.
- [15] R. Xu, H. Ji, K. Li, Y. Kang, and K. Yang, Relative position and attitude coupled control with finite-time convergence for spacecraft rendezvous and docking, 2015 IEEE 54th Annual Conference on Decision and Control (CDC) December 15-18, 2015, Osaka, Japan.
- [16] Y. Yang, Quaternion based model for momentum biased nadir pointing spacecraft, *Aerospace Science and Technology*, 14(3), 199-202, 2010.
- [17] Y. Yang, Quaternion based LQR spacecraft control design is a robust pole assignment design, *Journal of Aerospace Engineering*, Vol. 27, No. 1, 2014, pp. 168-176.
- [18] W.J. Rugh, and J.S. Shamma, Research on gain scheduling, *Automatica*, 36, 2000, pp. 1401-1425.
- [19] K.J. Astrom and B. Wittenmark. *Computer-controlled systems: theory and design*. Courier Corporation, 2013.
- [20] Y. Yang, Singularity-free model predictive spacecraft attitude regulation using a variable-speed control moment gyroscope model, accepted *IEEE Transactions on Aerospace and Electronic Systems*, available in arXiv:1612.06784v1.
- [21] R. C. Dorf, and R. H. Hishop, *Modern control systems*, 11th edition, Pearson Prentice Hall, Upper Saddle River, NJ, 2008.
- [22] A. Pandey, R. Schmid, T. Nguyen, Y. Yang, V. Sima and A. L. Tits, Performance Survey of Robust Pole Placement Methods, the 53rd IEEE Conference on Decision and Control, Los Angeles, December 15-17, 2014.
- [23] A.L. Tits, and Y. Yang, Globally convergent algorithms for robust pole assignment by state feedback, *IEEE Transactions on Automatic Control*, Vol. 41, 1996, pp. 1432-1452.
- [24] Y. Yang, Spacecraft attitude determination and control: Quaternion based method, *Annual Reviews in Control*, 36, 2012, 198-219.
- [25] M.J. Sidi, *Spacecraft Dynamics and Control: A Practical Engineering Approach*, Cambridge University Press, Cambridge, UK, 1997.
- [26] Y. Xu, A. Tatsch, N. G. Fitz-Coy., Chattering free sliding mode control for a 6 DOF formation flying mission, In *Proceedings of AIAA Guidance, Navigation, and Control Conference and Exhibit*, San Francisco, USA, AIAA, 2005, pp. 2005-6464.
- [27] F. Curti, M. Romano, R. Bevilacqua, Lyapunov-based thrusters selection for spacecraft control: analysis and experimentation, *Journal of Guidance, Control, and Dynamics* Vol. 33, No. 4, 2010, pp.198-219.

- [28] Y. Yang, Attitude control in spacecraft orbit-raising using a reduced quaternion model, *Advances in Aircraft and Spacecraft Science*, Vol. 1, No. 4, 2014, pp. 427-441.
- [29] W.J. Rugh, *Linear System Theory*, Prentice-Hall, Inc., Englewood Cliffs, New Jersey, 1993, pp.117-119.
- [30] Y. Yang, and A.L. Tits, On robust pole assignment by state feedback, *Proceedings of the American Control Conference*, 1993, pp. 2765-2766.
- [31] J.R. Wertz, *Spacecraft Attitude Determination and Control*, Dordrecht Kluwer, 1978.